UNIVERSITY OF FORWARD THINKING WESTMINSTER

IIR Wavelet Filter Banks for ECG Signal Denoising

Eminaga, Y., Coskun, A. and Kale, I.

https://doi.org/10.23919/SPA.2018.8563418

IIR Wavelet Filter Banks for ECG Signal Denoising

Yaprak Eminaga, Adem Coskun, and Izzet Kale
Applied DSP and VLSI Research Group
University of Westminster, London, W1W 6UW, United Kingdom
Email: y.eminaga@my.westminster.ac.uk, a.coskun@westminster.ac.uk, kalei@westminster.ac.uk

***Abstract*—ElectroCardioGram (ECG) signals are widely used for diagnostic purposes. However, it is well known that these recordings are usually corrupted with different type of noise/artifacts which might lead to misdiagnosis of the patient. This paper presents the design and novel use of Infinite Impulse Response (IIR) filter based Discrete Wavelet Transform (DWT) for ECG denoising that can be employed in ambulatory health monitoring applications. The proposed system is evaluated and compared in terms of denoising performance as well as the computational complexity with the conventional Finite Impulse Response (FIR) based DWT systems. For this purpose, raw ECG data from MIT-BIH arrhythmia database are contaminated with synthetic noise and denoised with the aforementioned filter banks. The results from 100 Monte Carlo simulations demonstrated that the proposed filter banks provide better denoising performance with fewer arithmetic operations than those reported in the open literature.**

***Keywords*—ECG denoising, Discrete Wavelet Transform, FIR wavelets, IIR wavelets.**

I. Introduction

The ECG signals are usually contaminated with various noise where the noise and signal spectra overlap and the conventional filtering techniques are insufficient to remove this noise. DWT is a popular tool in the field of non-stationary signal processing that provides simultaneous time and frequency information, and has been used to detect such overlapping noise. In ECG denoising literature a vast amount of research employed FIR filter banks with various wavelet families, most popular ones being the Daubechies such as $Haar$, $db2$, and $db4$, Symmlets and Coiflets [1]–[3]. On the other hand, IIR wavelet filter bank studies are less extensive and limited to image processing and compressing applications [4], [5]. This paper presents the design of IIR DWT filter banks and their novel application in ECG signal denoising. To the best knowledge of the authors', this is a first in the open literature and the results showed that the proposed IIR DWT filter banks achieve higher output Signal-to-Noise Ratio (SNR) and lower Mean Square Error (MSE) with reduced arithmetic operation complexity compared to the conventional FIR wavelets.

Section II provides brief information regarding the theory of IIR wavelet design followed by the details of the designed IIR wavelets. Section IV introduces the wavelet thresholding technique employed and the noisy test data generated. Comparative analysis on the noise suppression performance of the proposed IIR and FIR wavelets for different noise scenarios are presented in Section V. Finally, Section VI presents the conclusions.

II. IIR Wavelet Analysis Filter Bank Properties

The analysis part of a two channel Perfect Reconstruction (PR) IIR filter bank can be realized with a halfband lowpass and a halfband highpass filter denoted by $H_0(z)$ and $H_1(z)$, respectively. These filters are based on the parallel connection of two real all-pass filters [6], [7] and 1-level transform matrix for the analysis filter bank is given in (1).

$$\boldsymbol{H}\left(\boldsymbol{z}\right)=\begin{bmatrix}H_0\left(z\right)\\H_1\left(z\right)\end{bmatrix}=\frac{1}{\sqrt{2}}\begin{bmatrix}A_0\left(z^2\right)+z^{-1}A_1\left(z^2\right)\\A_0\left(z^2\right)-z^{-1}A_1\left(z^2\right)\end{bmatrix}, \quad (1)$$

where $A_0(z)$ and $A_1(z)$ are M^{th} order allpass filters with a general transfer function,

$$A\left(z\right)=z^{-M}\frac{\sum\limits_{m=0}^{M}\alpha_m z^m}{\sum\limits_{m=0}^{M}\alpha_m z^{-m}} \quad (2)$$

As it can be observed from (1), $H_0(z)$ and $H_1(z)$ are power complementary filters, since they satisfy the following property.

$$\left|H_0\left(z\right)\right|^2+\left|H_1\left(z\right)\right|^2=1 \quad (3)$$

The scaling and wavelet functions associated with the aforementioned filters, can be achieved by iterating the filter bank J times on its lowpass branch as shown in (4). This will result in transfer functions $\Phi\left(z\right)$ and $\Psi\left(z\right)$ with lowpass and bandpass spectrum where their impulse responses are the scaling ($\phi\left(n\right)$) and wavelet ($\psi\left(n\right)$) functions, respectively.

$$\begin{aligned}\Phi\left(z\right)&=\prod_{j=0}^{J-1}H_0\left(z^{2^j}\right)\\\Psi\left(z\right)&=H_1\left(z^{2^{j-1}}\right)\prod_{j=0}^{J-2}H_0\left(z^{2^j}\right)\end{aligned} \quad (4)$$

It is well known that, the regularity of wavelets defines the smoothness of the wavelet function and has a crucial effect for noise reduction applications. It is directly related to the wavelet's vanishing moments which is the number of times the wavelet spectrum vanishes (goes to zero) at $\omega = 0$ i.e $\left|\Psi(e^{j\omega})\right|_{\omega=0}=0$ where $z=e^{j\omega}$. Thus, the aforementioned $H_0\left(z\right)$ and $H_1\left(z\right)$ needs to be designed with an additional flatness condition as shown in (5) [8].

$$\left.\frac{\partial^k\left|H_1\left(e^{j\omega}\right)\right|}{\partial\omega^k}\right|_{\omega=0}=\left.\frac{\partial^k\left|H_0\left(e^{j\omega}\right)\right|}{\partial\omega^k}\right|_{\omega=\pi}=0 \quad (5)$$

for $k = 0, 1, ...K-1$, where K corresponds to the number of zeros of $H_1(z)$ at $z = 0$ and $H_0(z)$ at $z = -1$ i.e. Nyquist frequency. This design procedure can be reduced to the design of $H_0(z)$ due to the power complementary properties given in (3). For a given filter order, a trade of between frequency resolution and wavelet regularity exists. Therefore, it is critical to identify needs of the application and select the best possible frequency selectivity for a given flatness condition [6].

III. IIR Wavelet Analysis Filter Bank Design

In this study, IIR wavelet design methodology introduced by Zhang *et. al* [6] is adopted for implementing IIR wavelet filters with 3 and 5 vanishing moments and are referred to as $ilet3$ and $ilet5$, respectively in the rest of this document. Both wavelets filters are designed as maximally flat filters in order to achieve the maximum number of zeros at the Nyquist leading to the maximum possible smoothness of the scaling and wavelet functions. The number of vanishing moments are selected in order to closely match the most commonly used wavelet basis functions in ECG denoising applications including, $db2$, and $db4$ with 2 and 4 vanishing moments, respectively. Recalling (1), $H_0(z)$ can be re-written as,

$$H_0(z) = \frac{1}{2} A_0\left(z^2\right)\left(1 + z^{-1} U\left(z^2\right)\right) \tag{6}$$

where $U(z)$ is an allpass filter with a general transfer function given in (2). For $ilet5$ wavelets $U(z)$ is chosen to be a second order filter with real coefficients a_2, a_1, and $a_0 = 1$. Thus, for $M = 2$, its transfer function is expressed as,

$$U\left(z^2\right) = \frac{A_1\left(z^2\right)}{A_0\left(z^2\right)} = z^{-4} \frac{a_0 + a_1 z^2 + a_2 z^4}{a_0 + a_1 z^{-2} + a_2 z^{-4}} \tag{7}$$

The frequency response of $H_0(z)$ is calculated by evaluating (6) on the unit circle and the magnitude response is given by,

$$\left|H_0\left(e^{j\omega}\right)\right| = \cos\frac{\theta(\omega)}{2} \tag{8}$$

where $\theta(\omega)$ is the phase response of $z^{-1}U\left(z^2\right)$. Therefore, for $ilet5$, $\theta(\omega)$ and $\left|H_0\left(e^{j\omega}\right)\right|$ is respectively computed as,

$$\theta(\omega) = -2\tan^{-1}\frac{\sin\left(\frac{5\omega}{2}\right) + a_1\sin\left(\frac{\omega}{2}\right) - a_2\sin\left(\frac{3\omega}{2}\right)}{\cos\left(\frac{5\omega}{2}\right) + a_1\cos\left(\frac{\omega}{2}\right) + a_2\cos\left(\frac{3\omega}{2}\right)} \tag{9}$$

$$\left|H_0\left(e^{j\omega}\right)\right| = \frac{\cos\left(\frac{5\omega}{2}\right) + a_1\cos\left(\frac{\omega}{2}\right) + a_2\cos\left(\frac{3\omega}{2}\right)}{\sqrt{3 + 2a_1(1+a_2)\cos(2\omega) + 2a_2\cos(4\omega)}} \tag{10}$$

As mentioned before, the smoothness of the wavelet function is determined by the number of zeros at the Nyquist, which is computed by substituting the numerator of (10) into (5). Then, filter coefficients $a_1 = 10$ and $a_2 = 5$ are calculated by solving the linear equations obtained. The same steps are applied for $ilet3$ with $M = 1$ and $K = 3$. This results in $a_1 = 3$. Following (7), the poles of $U(z)$ that lies inside the unit circle corresponds to the poles of $A_1(z)$ and the poles outside the unit circle corresponds to the zeros of $A_0(z)$. By assigning the poles correctly, two stable allpass filters are obtained. The magnitude responses and pole-zero locations of

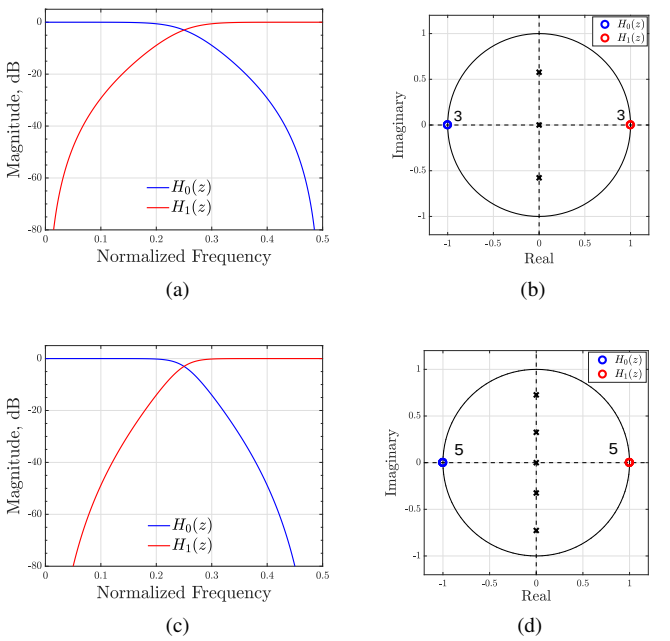

Fig. 1. $ilet3$; (a) Magnitude response and (b)Pole-Zero locations. $ilet5$; (c) Magnitude response and (d) Pole-Zero locations.

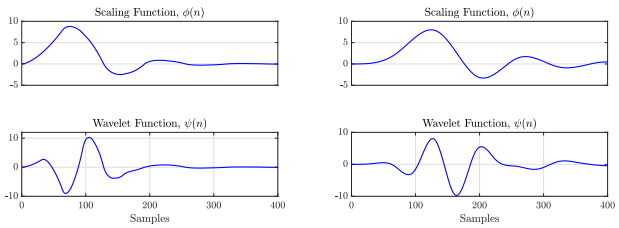

Fig. 2. Scaling ($\phi(n)$) and Wavelet ($\psi(n)$) functions of (a) $ilet3$ and (b) $ilet5$ after 8 iterations.

$H_0(z)$ and $H_1(z)$ and corresponding impulse responses, $\phi(n)$ and $\psi(n)$ for $ilet3$ and $ilet5$ are presented in Fig. 1 and Fig. 2, respectively.

IV. Method

There is various types of noise such as powerline interference, baseline wander, and muscle contraction artifacts that are assumed to be additive and independent from the the ECG signal which is generally modelled as $x_n(n) = x_c(n) + e(n)$, where $x_n(n)$, $x_c(n)$, and $e(n)$ are the noisy ECG, clean ECG and composite noise, respectively. Although powerline interference can be eliminated by a digital notch filter, the spectrum of other noise sources overlap with the spectrum of the ECG signal. In such circumstances, wavelet thresholding can be employed where the noisy signal is decomposed into several levels, denoised and reconstructed [9]. For this study, the noisy ECG signal is decomposed into 7 levels and each of the detail coefficients (i.e. outputs of $H_1(z)$ at each level) are thresholded using the soft thresholding method, in

which the threshold is computed using the Rigorous SURE (Stein's Unbiased Risk Estimator) criterion [10]. The baseline wander is removed by nullifying the finest level approximation coefficients (i.e. $H_0(z)$ output at level 7) and the denoised signal is reconstructed from the thresholded detail coefficients. The thresholding method and threshold criterion is empirically determined where soft thresholding is well-known for delivering smoother outputs and the Rigorous SURE threshold selection scheme is known for successfully identifying the small details of signal overlapped with noise. A good comparison of different threshold selection and thresholding methods can be found in [11].

A. Generated ECG data and Synthetic Noise Sources

Four raw ECG records ('103', '105', '109', and '118') are randomly taken from the MIT-BIH arrhythmia database which are resampled to 256 Hz. In order to obtain clean control data, preprocessing stages are applied, including notch and highpass filtering (cut-off frequency (f_c) = 0.5 Hz), to remove 60 Hz powerline interference and baseline wander, respectively. Then, the ElectroMyogram (EMG) interference ($x_e(n)$) is modelled as white Gaussian noise, whereas the baseline wander is modelled as additive combination of deterministic and random data with frequency content below 1 Hz as shown in (11).

$$x_{bw}(n) = \sum_{i=1}^{P} \sin\left(2\pi n \frac{f_i}{f_s}\right) + W(n) \tag{11}$$

where $0 < f_i \leq 1$ for $i = 1, 2, \ldots, P$, f_s is the sampling frequency and $W(n)$ is lowpass filtered (f_c = 1 Hz) white Gaussian noise. Thus, the composite noise is obtained by $e(n) = A(x_e(n) + x_{bw}(n))$ where A is the input noise scaling factor that is determined by the desired input SNR and is computed via;

$$A = \sqrt{\frac{\sum_{n=1}^{N} |x_c(n)|^2}{\sum_{n=1}^{N} |e(n)|^2} 10^{-\text{SNR}/10}} \tag{12}$$

B. Quantitative Evaluation

The ECG signal denoising performance of $ilet3$ and $ilet5$ as well as $Haar$, $db2$, $db4$, $sym4$, and $coif2$ wavelet filter banks are evaluated and compared by computing the SNR improvement and MSE which are obtained from;

$$\begin{aligned} \text{SNR}_{imp} &= \frac{\sum_{n=1}^{N} |x_n(n) - x_c(n)|^2}{\sum_{n=1}^{N} |x_d(n) - x_c(n)|^2} \\ \text{MSE} &= \frac{1}{N} \sum_{n=1}^{N} |x_d(n) - x_c(n)|^2 \end{aligned} \tag{13}$$

where $x_d(n)$ is the denoised ECG signal.

V. Results and Discussions

Four records ('103', '105', '109', and '118') are contaminated by adding the synthetically generated EMG and baseline wander with SNR ranging from -12 to 20 dB. Fig. 3

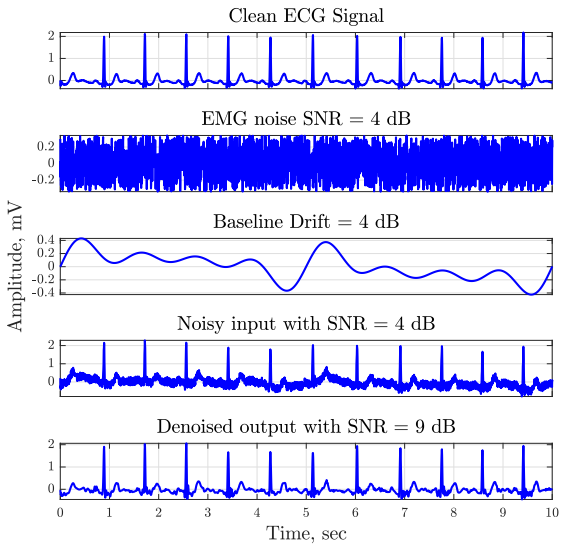

Fig. 3. Top to bottom;10 seconds of clean record '103',EMG noise, Baseline Wander, Noisy ECG, and Denoised ECG.

presents (top to bottom) the clean ECG record '103', generated synthetic EMG and baseline wander, noisy ECG contaminated with composite noise with $SNR = 4$ dB, and finally the denoised ECG with $ilet5$ wavelet filter bank. For each data record and at each SNR, 100 Monte Carlo Simulations are performed and the average SNR and MSE are computed. Results for the noisy record '103' are shown in Fig. 4. As it can be observed, the $ilet5$ wavelet filter bank provides the highest SNR improvement and the lowest MSE when compared to others, where $ilet3$ provides the second best results. In Table I, the average SNR improvement (in dB) figures obtained for $ilet3$, $ilet5$, $db4$ and $Haar$ wavelets are also presented for four noisy ECG records. As expected, $ilet5$ provides the best results compared to the FIR wavelets, followed by $ilet3$ both under high and relatively low noise power. This is due to the better frequency selectivity achieved with the IIR wavelets despite having lower vanishing moments,i.e. in the $ilet3$ case. Although, $Haar$ wavelet is the simplest FIR wavelet filter which makes it desirable for power limited applications, it achieves the lowest denoising performance. On the other hand, $ilet3$ filter with one distinct coefficient provides better denoising performance making it a favourable choice amongst the others. For applications where the denoising performance is critical and the power consumption can be compromised then the $ilet5$ can be employed which uses only two distinct coefficients. In addition, Table II presents the average MSE results where the $ilet5$ and $ilet3$ wavelets provide the two minimum MSE results. This is an indication of a relatively smaller signal distortion after denoising which is a significant factor for diagnostic applications. In terms of computational complexity except from the $Haar$ filter, rest of the FIR filters employ 4, 8 and 12 rational coefficients. Thus, based on the selected filter structure, the arithmetic and storage complexity

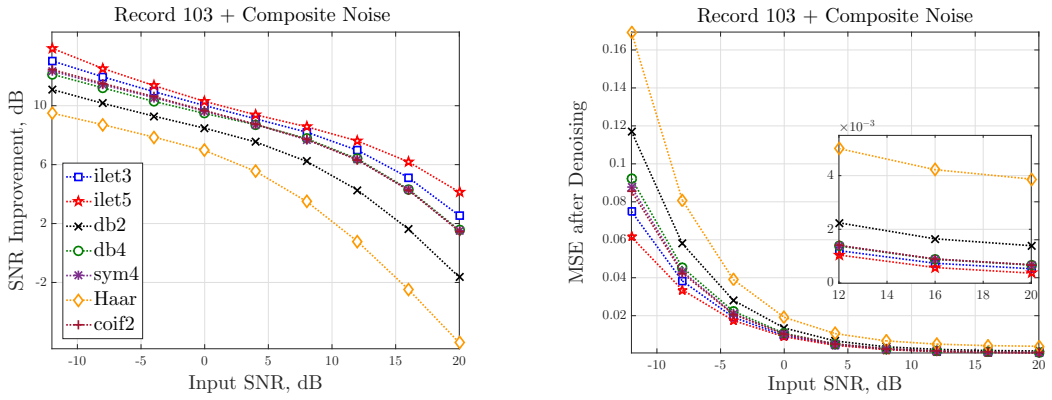

(a) (b)

Fig. 4. Average (a) SNR Improvement (dB), and (b) MSE, after wavelet denoising with $ilet3$, $ilet5$, $db2$, $db4$, $sym4$, $Haar$ and $coif2$.

TABLE I
SNR IMPROVEMENT AFTER WAVELET DENOISING.

	Input SNR = -12 dB				Input SNR = 4 dB			
	$ilet3$	$ilet5$	$db4$	$Haar$	$ilet3$	$ilet5$	$db4$	$Haar$
'103'	13.07	**13.92**	12.18	9.49	9.13	**9.4**	8.72	5.55
'105'	13.71	**14.58**	12.72	9.67	9.21	**9.90**	8.72	5.32
'109'	13.92	**14.92**	12.98	9.68	10.18	**11.38**	9.20	5.27
'118'	13.68	**14.42**	12.56	9.61	8.24	**9.34**	6.93	4.72

TABLE II
MSE AFTER WAVELET DENOISING

	Input SNR = -12 dB				Input SNR = 4 dB			
	$ilet3$	$ilet5$	$db4$	$Haar$	$ilet3$	$ilet5$	$db4$	$Haar$
'103'	0.07	**0.06**	0.09	0.17	0.0046	**0.0044**	0.005	0.011
'105'	0.06	**0.05**	0.07	0.16	0.0045	**0.0038**	0.0049	0.011
'109'	0.12	**0.098**	0.15	0.17	0.0074	**0.0056**	0.0086	0.022
'118'	0.11	**0.096**	0.14	0.29	0.0101	**0.0078**	0.0129	0.022

will always be higher for the FIR wavelets in comparison to the IIR wavelets. Also, it is a well known fact that for fixed-point implementations, FIR filters are more sensitive to coefficient quantization which require higher word-lengths compared to allpass based halfband polyphase IIR filters, further increasing the system complexity.

VI. CONCLUSIONS

In this paper, the novel use of IIR wavelet filter banks for ECG signal denoising is presented. For this purpose, two maximally flat and stable IIR wavelet filters, $ilet3$ and $ilet5$ are designed. Both filters are computationally efficient where $ilet3$ and $ilet5$ employs one and two distinct coefficients, respectively that can be implemented with simple shift and add operations without using costly multipliers. A comparative analysis of ECG signal denoising based on the aforementioned IIR wavelet filters and state-of-the-art FIR wavelet filters is carried out. The denoising performance of all filter banks are evaluated through the generation of the synthetic noisy signals and compared by means of the SNR improvement and the output MSE. The results obtained demonstrated that the IIR wavelets achieve the best ECG denoising performance with the least signal distortion amongst the others with fewer arithmetic operations. This study demonstrates that IIR wavelets can be included in more sophisticated denoising applications in portable devices due to their better frequency selectivity with lesser arithmetic operations.

ACKNOWLEDGMENT

The authors wish to thank the University of Westminster Faculty of Science and Technology for the PhD Studentship.

REFERENCES

[1] Y. Eminaga, A. Coskun, and I. Kale, "Multiplier Free Implementation of 8-tap Daubechies Wavelet Filters for Biomedical Applications," in *2017 New Generation of CAS (NGCAS)*. IEEE, 2017, pp. 129–132.

[2] S. Nagai, D. Anzai, and J. Wang, "Motion artefact removals for wearable ECG using stationary wavelet transform," *Healthcare technology letters*, vol. 4, no. 4, p. 138, 2017.

[3] P. Shemi and E. Shareena, "Analysis of ECG signal denoising using discrete wavelet transform," in *Engineering and Technology (ICETECH), 2016 IEEE International Conference on*. IEEE, 2016, pp. 713–718.

[4] X. Zhang, W. Wang, T. Yoshikawa, and Y. Takei, "Design of IIR orthogonal wavelet filter banks using lifting scheme," *IEEE Transactions on Signal Processing*, vol. 54, no. 7, pp. 2616–2624, 2006.

[5] J. M. Abdul-Jabbar and R. W. Hmad, "Allpass-based design, multiplierless realization and implementation of IIR wavelet filter banks with approximate linear phase," in *Innovation in Information & Communication Technology (ISIICT), 2011 Fourth International Symposium on*. IEEE, 2011, pp. 118–123.

[6] X. Zhang and T. Yoshikawa, "Design of orthonormal IIR wavelet filter banks using allpass filters," *Signal Processing*, vol. 78, no. 1, pp. 91–100, 1999.

[7] S. Damjanovic and L. Milic, "Examples of orthonormal wavelet transform implementad with IIR filter pairs," *Proc. SMMSP 2005, Riga, Latvia*, pp. 19–27, 2005.

[8] C. Herley and M. Vetterli, "Wavelets and recursive filter banks," *IEEE Transactions on Signal Processing*, vol. 41, no. 8, pp. 2536–2556, 1993.

[9] J. Gao, H. Sultan, J. Hu, and W.-W. Tung, "Denoising nonlinear time series by adaptive filtering and wavelet shrinkage: a comparison," *IEEE Signal Processing Letters*, vol. 17, no. 3, pp. 237–240, 2010.

[10] D. L. Donoho and I. M. Johnstone, "Adapting to unknown smoothness via wavelet shrinkage," *Journal of the American Statistical Association*, vol. 90, no. 432, pp. 1200–1224, 1995.

[11] S. R. Messer, J. Agzarian, and D. Abbott, "Optimal wavelet denoising for phonocardiograms," *Microelectronics Journal*, vol. 32, no. 12, pp. 931–941, 2001.